Engineering Structures 138 (2017) 434–446

Contents lists available at ScienceDirect

Engineering Structures

journal homepage: www.elsevier.com/locate/engstruct

A generalized analytical model for sloped rolling-type seismic isolators

Shiang-Jung Wang, Chung-Han Yu, Wang-Chuen Lin, Jenn-Shin Hwang, Kuo-Chun Chang *

Department of Civil Engineering, National Taiwan University, Taiwan

ARTICLE INFO

Article history:
Received 29 December 2015
Revised 13 December 2016
Accepted 15 December 2016

Keywords:
Sloped rolling-type seismic isolator
Generalized analytical model
Equipment
Seismic performance
Vertical excitation

ABSTRACT

The exact and simplified generalized analytical models for the sloped rolling-type seismic isolator in which two V-shaped surfaces in contact with cylindrical rollers are designed with arbitrary sloping angles are proposed. Numerical predictions are compared with horizontal seismic simulation test results to demonstrate the accuracy and practicability of the proposed simplified model. Furthermore, the influences arising from two simplification assumptions on the horizontal acceleration prediction are numerically examined. The results indicate that the effect of vertical acceleration excitation plays a more crucial role in prediction accuracy and conservative design compared to that of higher order terms of sloping angles.

© 2017 Elsevier Ltd. All rights reserved.

1. Introduction

Rolling-based metallic seismic isolators [1] in which either a ball rolls on flat [2], concave [3–5], or conical [6] surfaces or a rod rolls on flat [7,8], curved [9–11], or sloped [12–15] surfaces (or rails) have been numerically and experimentally demonstrated for their excellent seismic isolation performance. Since the rolling friction force and the restoring force contributed by additional springs or due to gravity are very limited and much smaller than the input seismic force, the rolling motion can be activated immediately once an earthquake occurs, and the horizontal acceleration transmitted to the protected object can be significantly reduced during an earthquake. The seismic isolators, except those designed with flat surfaces in contact with balls or rods, have an inherent gravity-based self-centering capability after excitation.

Among various types of rolling-based metallic seismic isolators, the sloped rolling-type seismic isolators discussed in Lee et al.'s [13,14] and Wang et al.'s [15] studies attracted sustained attention. In addition to possessing the advantages aforementioned, the design of constant sloping surfaces in contact with cylindrical rollers can ensure that the horizontal acceleration transmitted to the protected object remains essentially constant regardless of any intensity and frequency content of excitation. Thus, the seismic isolators do not have a fixed vibration natural period, and can offer maximum horizontal decoupling between the protected object and input excitation. It is noteworthy that the zero post-elastic stiffness performance, i.e. the constant transmitted horizontal acceleration performance, is the most attractive feature. This feature can make the seismic isolators easily meet the rigorous performance-based design requirements for structural and non-structural systems if the maximum transmitted acceleration response is selected as the seismic performance criterion. Furthermore, to have a better displacement control and more effectively stop rolling motion respectively during and after excitation, the built-in damping mechanism provided by additional sliding friction was employed in these two studies. The normal force for the sliding friction was provided by screws in Lee et al.'s study, while that was provided by springs in Wang et al.'s study.

As shown in the schematic drawing of Fig. 1, the sloped rolling-type seismic isolators discussed in Lee et al.'s and Wang et al.'s studies were basically composed of three bearing plates (denoted as upper, intermediate, and lower bearing plates hereafter) and cylindrical rollers. In Lee et al.'s study, the upper and lower bearing plates were designed with flat surfaces in contact with the rollers, while the intermediate bearing plate was designed with V-shaped surfaces. In Wang et al.'s study, the three bearing plates were designed with V-shaped surfaces in contact with the rollers, and the sloping angles of the V-shaped surfaces were identical. Without considering the effects arising from higher order terms of sloping angles and vertical excitation, the dynamic behavior of a cylinder moving between a flat surface and a V-shaped surface along each principle horizontal direction was focused in Lee et al.'s study, while that between two V-shaped surfaces designed with the same sloping angle was concentrated in Wang et al.'s study. Because of different designs of rolling surfaces, the compatibility conditions in these two studies were diverse. Hence, the simplified equations of motion derived in these two studies were

* Corresponding author.
E-mail address: ciekuo@ntu.edu.tw (K.-C. Chang).

http://dx.doi.org/10.1016/j.engstruct.2016.12.027
0141-0296/© 2017 Elsevier Ltd. All rights reserved.

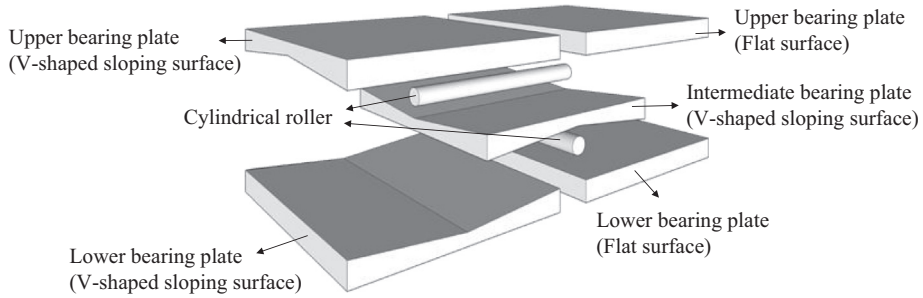

Fig. 1. Schematic drawings of sloped rolling-type seismic isolators discussed in Lee et al.'s [13,14] and Wang et al.'s [15] studies.

essentially different and cannot be exchanged. In addition, other refinements such as the multi-roller and pounding prevention mechanisms were developed in Wang et al.'s study. The multi-roller design can have a better stability performance compared with the conventional single-roller design. The design of an arc rolling range with a fixed curvature radius at the intersection of two inclines of V-shaped surfaces of bearing plates can effectively prevent pounding between rollers and inclined surfaces when rollers are passing through here. In Wang et al.'s study, a simplified analytical model was provided to fully describe the hysteretic behavior of the sloped rolling-type seismic isolator based on a combination of multi-linear elastic and plastic models. It is also mentioned here that the application purposes of Lee et al.'s and Wang et al.'s studies were bridge structures and equipment or facilities, respectively.

Therefore, this study first aims to derive generalized equations of motion for the sloped rolling-type seismic isolator in which the cylindrical rollers move between two V-shaped surfaces designed with arbitrary sloping angles. The design is different from and more generalized than Lee et al.'s and Wang et al.'s. The proposed simplified generalized analytical model, of course, is capable of describing the dynamic behavior of the two specific designs respectively discussed in Lee et al.'s and Wang et al.'s studies. The accuracy and practicability of the simplified model are verified by comparing with horizontal shaking table test results. Finally, by further comparing the numerical results predicted by the exact generalized analytical model with those by the simplified one, the influences caused by two simplification assumptions—neglect of higher order terms of sloping angles and vertical excitation—on the transmitted horizontal acceleration responses of the seismic isolator are thoroughly examined. It has never been discussed in detail before.

2. Derivation of generalized equations of motion

A simplified model, a cylindrical roller sandwiched between two V-shaped surfaces designed with different sloping angles θ_1 and θ_2, to represent the dynamic behavior of the sloped rolling-type seismic isolator in one principle horizontal direction as well as in the vertical direction is illustrated in Fig. 2(a), in which M, m_1, and m_2 are the seismic reactive masses of the protected object, superior bearing plate, and roller, respectively; r is the radius of the roller; and θ_1 and θ_2 are the sloping angles of the superior and inferior bearing plates, respectively. The following basic assumptions are made first for deriving the generalized equations of motion of the sloped rolling-type seismic isolator: (1) the roller and bearing plates are ideally contact and in pure rolling motion without any undesired sliding and overturning motions; (2) the rolling motions of the rollers between two bearing plates along two principle horizontal directions are identical; (3) an appropriate rigid-plastic hysteretic model (i.e. the Coulomb friction law) is employed to represent the force-displacement relationship of built-in damping behavior; (4) the inferior bearing plate is fixed to a rigid base; and (5) the payload of a to-be-protected object is applied on the superior bearing plate.

Two opposite rolling motion directions are identified by $\mathrm{sgn}(\dot{x}_1)=\mathrm{sgn}(\dot{x}_2)=1$ and $\mathrm{sgn}(\dot{x}_1)=\mathrm{sgn}(\dot{x}_2)=-1$ corresponding to the rightward $(\mathrm{sgn}(x_1)=\mathrm{sgn}(x_2)=1)$ and leftward $(\mathrm{sgn}(x_1)=\mathrm{sgn}(x_2)=-1)$ movements of the superior bearing plate (or the roller) relative to the inferior bearing plate. The free body diagrams for one of the four situations, $\mathrm{sgn}(x_1)=\mathrm{sgn}(x_2)=1$ and $\mathrm{sgn}(\dot{x}_1)=\mathrm{sgn}(\dot{x}_2)=1$, are shown in Fig. 2(b), in which $\ddot{x}_g(\ddot{z}_g)$ is the horizontal (vertical) acceleration excitation; $x_1(z_1)$, $\dot{x}_1(\dot{z}_1)$, and $\ddot{x}_1(\ddot{z}_1)$ are the horizontal (vertical) displacement, velocity, and acceleration responses of the protected object and superior bearing plate relative to the origin O, respectively; $x_2(z_2)$, $\dot{x}_2(\dot{z}_2)$, and $\ddot{x}_2(\ddot{z}_2)$ are the horizontal (vertical) displacement, velocity, and acceleration responses of the roller relative to the origin O, respectively; the positive directions of x and z are correspondingly defined to be rightward and upward in the figure; g is the acceleration of gravity; I is the moment of inertia of the roller; α is the angular acceleration of the roller (the positive rotation is defined to be clockwise in the figure); $f_1(f_2)$ and $N_1(N_2)$ are the rolling friction force and normal force acting between the superior bearing plate and roller (between the roller and inferior bearing plate), respectively; and F_D is the built-in friction damping force acting parallel to the slope of the bearing plates.

By considering the free body diagrams of the superior bearing plate and protected object, two dynamic force equilibrium equations are obtained as

$$-F_D\cos\theta_1\mathrm{sgn}(\dot{x}_1)-N_1\sin\theta_1\mathrm{sgn}(x_1)-f_1\cos\theta_1\mathrm{sgn}(\dot{x}_1)=(M+m_1)(\ddot{x}_1+\ddot{x}_g) \tag{1}$$

$$-F_D\sin\theta_1\mathrm{sgn}(x_1)\mathrm{sgn}(\dot{x}_1)+N_1\cos\theta_1-Mg-f_1\sin\theta_1\mathrm{sgn}(x_1)\mathrm{sgn}(\dot{x}_1)-m_1g=(M+m_1)(\ddot{z}_1+\ddot{z}_g) \tag{2}$$

Moreover, by considering the free body diagram of the roller, two dynamic force equilibrium and one dynamic moment equations are obtained as

$$F_D\cos\theta_1\mathrm{sgn}(\dot{x}_1)-F_D\cos\theta_2\mathrm{sgn}(\dot{x}_1)+N_1\sin\theta_1\mathrm{sgn}(x_1)-N_2\sin\theta_2\mathrm{sgn}(x_1)+f_1\cos\theta_1\mathrm{sgn}(\dot{x}_1)-f_2\cos\theta_2\mathrm{sgn}(\dot{x}_1)=m_2(\ddot{x}_2+\ddot{x}_g) \tag{3}$$

$$F_D\sin\theta_1\mathrm{sgn}(x_1)\mathrm{sgn}(\dot{x}_1)-F_D\sin\theta_2\mathrm{sgn}(x_1)\mathrm{sgn}(\dot{x}_1)-N_1\cos\theta_1+N_2\cos\theta_2+f_1\sin\theta_1\mathrm{sgn}(x_1)\mathrm{sgn}(\dot{x}_1)-f_2\sin\theta_2\mathrm{sgn}(x_1)\mathrm{sgn}(\dot{x}_1)-m_2g=m_2(\ddot{z}_2+\ddot{z}_g) \tag{4}$$

$$f_1r\mathrm{sgn}(\dot{x}_1)+f_2r\mathrm{sgn}(\dot{x}_1)=I\alpha \tag{5}$$

where $I=(1/2)m_2r^2$.

Download English Version:

https://daneshyari.com/en/article/4920342

Download Persian Version:

https://daneshyari.com/article/4920342

Daneshyari.com